Muniyappa, K., Shaner, S. L., Tsang, S. S., & Radding, C. M. (1984) *Proc. Natl. Acad. Sci. U.S.A. 81*, 2757–2761.
Neuhard, J., & Thomassen, E. (1971) *Eur. J. Biochem. 20*, 36–43.
Phizicky, E. M., & Roberts, J. W. (1981) *Cell 25*, 259–267.
Pugh, B. F., & Cox, M. M. (1987) *J. Biol. Chem. 262*, 1326–1336.
Pugh, B. F., & Cox, M. M. (1988) *J. Biol. Chem. 263*, 76–83.
Resnick, J., & Sussman, R. (1982) *Nucleic Acids Res. 10*, 5239–5253.
Roberts, J. W., Phizicky, E. M., Burbee, D. G., Roberts, C. W., & Moreau, P. L. (1982) *Biochimie 64*, 805–807.
Roman, L. J., & Kowalczykowski, S. C. (1986) *Biochemistry 25*, 7375–7385.
Schutte, B. C., & Cox, M. M. (1987) *Biochemistry 26*, 5616–5625.
Tsang, S. S., Chow, S. A., & Radding, C. M. (1985) *Biochemistry 24*, 3226–3232.
Tsang, S. S., Muniyappa, K., Azhderian, E., Gonda, D. K., Radding, C. M., Flory, J., & Chase, J. W. (1985) *J. Mol. Biol. 185*, 295–309.
Uhlin, B. E., & Clark, A. J. (1981) *J. Bacteriol. 148*, 386–390.
Uhlin, B. E., Schweikart, V., & Clark, A. J. (1983) *Gene 22*, 255–265.
Weinstock, G. M. (1982) *Biochimie 64*, 611–617.
Weinstock, G. M., McEntee, K., & Lehman, I. R. (1981) *J. Biol. Chem. 256*, 8829–8834.

Thermodynamic Comparison of the Base Pairs Formed by the Carcinogenic Lesion O^6-Methylguanine with Reference both to Watson–Crick Pairs and to Mismatched Pairs†

Barbara L. Gaffney and Roger A. Jones*
Department of Chemistry, Rutgers—The State University of New Jersey, Piscataway, New Jersey 08855
Received December 27, 1988; Revised Manuscript Received March 22, 1989

ABSTRACT: A set of 10 non-self-complementary nonadeoxyribonucleoside octaphosphates, d(GGTTXTTGG) and d(CCAAYAACC), where X and Y are A, C, G, T, or O⁶MeG, has been synthesized by a large-scale, automated, phosphoramidite procedure. Purification was effected by reversed-phase HPLC, and the base composition was verified by analytical HPLC after enzymatic degradation to the constituent deoxynucleosides. This set of molecules was designed to allow evaluation of the nearest-neighbor dependence of each base pair. The thermal stability, expressed as T_{max}, of each duplex containing one of the O⁶MeG base pairs, a Watson–Crick pair, or one of the mismatches possible with this set of molecules was determined over a concentration range of 5.7–200 μM. From these data the $\Delta H°$, $\Delta S°$, and $\Delta G°$ of each combination were calculated. In general, the relative thermal stabilities observed for the O^6-methylguanine combinations confirm our previous findings that the most stable base pair is formed with cytosine rather than thymine and that all O⁶MeG pairs are much weaker than Watson–Crick base pairs [Kuzmich, S., Marky, L. A., & Jones, R. A. (1983) *Nucleic Acids Res. 11*, 3393–3404; Gaffney, B. L., Marky, L. A., & Jones, R. A. (1984) *Biochemistry 23*, 5686–5691]. Moreover, the nine combinations containing O^6-methylguanine are all of similar thermal stability, cover a much smaller range in T_{max} than do the mismatches, and show little sequence dependence.

The generation of O^6-alkylguanine lesions in DNA has been implicated as an initiatory molecular event both to mutagenesis and to some types of carcinogenesis (Grunberger & Singer, 1983). For example, a single exposure of Buf/N rats to the methylating agent and carcinogen *N*-nitroso-*N*-methylurea (NMU) is sufficient to initiate malignancy and has been shown to produce a transforming Ha-ras-1 gene containing a specific G → A transition mutation (Zarbl et al., 1985). Moreover, low doses of the carcinogen 4-(*N*-methyl-*N*-nitrosoamino)-1-(3-pyridyl)-1-butanone (NNK), a major nitrosamine present in tobacco, which give rise to a high incidence of malignant lung tumors, also correlate with specific formation of O⁶MeG in lung Clara cells (Belinsky et al., 1987).

In human cell lines with low levels of the alkyltransferase required for repair of O⁶MeG, an increased sensitivity to the lethal and mutagenic effects of *N*-methyl-*N'*-nitrosoguanidine (MNNG) was observed (Domoradzki et al., 1984). Similarly, the leukemic transformation of rapidly proliferating bone marrow cells, induced by nitrosoureas, has been associated with their low levels of alkyltransferase (Gerson et al., 1987). Patients suffering from autoimmune diseases have also been found to be deficient in removal of O⁶MeG (Lawley, 1986).

It is known from experiments in which an oligonucleotide containing O⁶MeG was inserted into a viral or plasmid genome that O⁶MeG brings abount exclusively a G → A transition (Loechler et al., 1984; Chambers et al., 1985; Hill-Perkins et al., 1986; Bhanot et al., 1986; Topal et al., 1986). In addition, although the DNA sequence was shown to play a role in the *extent* of alkylation by NMU (Briscoe et al., 1985), the resulting mutations are always G → A (Richardson et al., 1987; Lucchesi et al., 1986). This strong preference for G → A transitions is consistent with the preferential pairing of O⁶MeG with thymine first postulated by Loveless (1969) and later supported on theoretical grounds (Klopman et al., 1982; Nagata et al., 1982). A later molecular mechanical simulation, however, concluded that there should be little or no difference in stability between O⁶MeG·C and O⁶MeG·T pairs (Caldwell & Kollman, 1985).

† This work was supported by NIH Grant GM 31483, American Cancer Society Grant CA 248B, an American Cancer Society Faculty Research Award to R.A.J., and the Busch Memorial Fund.

0006-2960/89/0428-5881$01.50/0

We have previously examined two groups of duplexes containing O^6MeG residues: the two hexamers d[CGC(O^6Me)GCG] and d[CGT(O^6Me)GCG] (Kuzmich et al., 1983) and the four dodecamers d[CGNGAATTC(O^6Me)GCG], where N = A, C, G, or T (Gaffney et al., 1984a). Contrary to our original expectations, the duplexes with O^6MeG·T pairing, or potential pairing, proved to be the least thermally stable of the duplexes in each set. Analysis of the dodecamers by proton NMR indicated that the O^6MeG·N pairs were not looped out of the duplex and therefore could be stacked (Patel et al., 1986a–c). However, the only information about H-bonding that could be obtained for any of the O^6MeG·N pairs was from the chemical shift of the thymine N^3 proton, which appeared at ~9 ppm. This is several ppm upfield of the chemical shift range for thymine in an A·T Watson–Crick pair, perhaps indicative of the presence of a weak or distorted H-bond or the absence of H-bonding to this proton. The present work was designed to explore duplexes in which the O^6MeG was surrounded by A·T pairs in order to determine whether our earlier results were somehow limited to the particular families studied, where O^6MeG was always flanked by C, or were generally true for O^6MeG.

Materials and Methods

Aminopropyl-derivatized controlled pore glass (CPG) was purchased from Electro-Nucleonics, Fairfield, NJ, and loaded with succinylated nucleosides as reported previously for polystyrene (Gaffney et al., 1984b). Unmodified deoxynucleosides were protected as described previously (Ti et al., 1982), and N^2-acetyl-O^6-methyl-2′-deoxyguanosine was synthesized as reported earlier (Gaffney et al., 1984a). Pyridine, triethylamine, and diisopropylamine were dried by distillation from calcium hydride. The acetonitrile was dried over 3-Å molecular sieves. Solvents used for oligonucleotide synthesis were all of HPLC grade and were purchased from Fisher Scientific; reagents were purchased from Aldrich Chemical Co. Venom phosphodiesterase and alkaline phosphatase were obtained from Sigma. The falling-film distillation apparatus was obtained from Kontes or Aldrich.

2-Cyanoethyl N,N,N′,N′-Tetraisopropylphosphorodiamidite. To 61 mL of freshly distilled phosphorus trichloride (0.70 mol) dissolved in 300 mL of anhydrous diethyl ether (previously dried over molecular sieves), which was stirred mechanically under a N_2 atmosphere and maintained at −30 °C, was added dropwise over 2 h a mixture of 57 mL (0.70 mol) of pyridine, 48 mL (0.70 mol) of freshly distilled 3-hydroxypropionitrile, and 50 mL of anhydrous diethyl ether. The cooling bath was removed, and the mixture was stirred for 18 h under a small positive N_2 pressure. The ether solution was transferred under N_2 pressure with filtration into a dry flask. The remaining pyridinium hydrochloride was washed twice with 100-mL portions of anhydrous diethyl ether which was transferred as above. The solution was concentrated on a rotary evaporator, and the resulting liquid was distilled under vacuum (500–1000 mT) with a falling-film distillation apparatus with refluxing ethyl acetate as the heat source to give 70 g (0.41 mol, 58%) of 2-cyanoethyl dichlorophosphite. The ^{31}P NMR ($CDCl_3$) showed a single peak at 178.8 ppm (reference 85% H_3PO_4).

To 28 g (163 mmol) of this compound dissolved in 300 mL of anhydrous diethyl ether and stirred under N_2 at −20 °C was added dropwise 96 mL (685 mmol, 4.2 equiv) of diisopropylamine. The ice bath was removed, and the mixture was stirred for 1 h. The ether solution was transferred with filtration under N_2 pressure to a dry flask. The remaining salt was washed twice with 70-mL portions of anhydrous ether, which was transferred as above. The solution was concentrated on a rotary evaporator and filtered into a small, dry flask. The liquid was stirred under vacuum for 20 min and then distilled under vacuum (400–500 mT) with the falling-film distillation apparatus with refluxing toluene as the heat source to give 18.5 g (61 mmol, 37% yield) of clear, colorless product. The ^{31}P NMR ($CDCl_3$) spectrum showed a single peak at 123.6 ppm (reference 85% H_3PO_4).

Synthesis of Cyanoethyl Phosphoramidites. To 5.0 mmol of the appropriately protected nucleoside and 175 mg (2.5 mmol) of sublimed tetrazole in 25 mL of dry acetonitrile was added 0.49 mL (3.5 mmol) of diisopropylamine followed after 5 min by 1.8–2.1 mL (5.5–6.5 mmol) of 2-cyanoethyl *N,N,N′,N′*-tetraisopropylphosphorodiamidite. After 1 h, the mixture was partitioned between 200 mL of 5% aqueous $NaHCO_3$ and 200 mL of methylene chloride. The organic layer was washed with a 100-mL portion of water and was then concentrated to a gum. The crude product was purified by flash chromatography on silica gel using a step gradient of 10–25% ethyl acetate in methylene chloride. The appropriate fractions were combined and evaporated to a solid foam.

Oligonucleotide Synthesis and Deprotection. The oligomers were prepared on a Biosearch Model 8600 DNA synthesizer on a scale of ~20 μmol. The CPG-bound nucleoside (450 mg, 20 μmol) was treated sequentially with the following: (1) 2% dichloroacetic acid in methylene chloride, for either 1 min (purines) or 2.5 min (pyrimidines); (2) a freshly prepared solution of 0.16 M tetrazole in acetonitrile (20–32 equiv) and 0.04 M phosphoramidite in acetonitrile (5–8 equiv) for 10–15 min; (3) a freshly prepared oxidizing solution made of 0.016 M I_2 in 89% tetrahydrofuran (THF), 10% water, and 1% pyridine for 30 s; (4) a capping mixture containing 5% (dimethylamino)pyridine (DMAP), 5% pyridine, 8% acetic anhydride, and 82% THF for 11 s. The support was washed extensively with acetonitrile between each step.

At the end of the synthesis, the unmodified oligomers were shaken with concentrated, aqueous ammonia for 3 days and then partially concentrated and lyophilized. Oligomers containing O^6-methyldeoxyguanosine were treated with 10% diazabicycloundecene (DBU) in methanol for 5 days; the solution was then neutralized with ammonium chloride and concentrated.

Oligonucleotide Purification. Analytical HPLC was performed using a Novapak C_{18} cartridge in a Waters Z module or a Beckman Ultrapure C_3 column. Two Waters M6000A pumps, a Model 660 solvent programmer and Model 440 UV detector were employed. Preparative HPLC was done using the indicated columns with the same system except that an Altex 153 detector with a preparative flow cell was used.

The two oligomers containing O^6-methyldeoxyguanosine were first desalted on a Rainin 2.5 cm × 10 cm C_{18} cartridge. The sample was loaded in 2% acetonitrile–0.1 M ammonium bicarbonate (ABC), washed with 50 mL of the same solution, and eluted from the column with a gradient of 2–20% acetonitrile–0.1 M ABC in 10 min at 2 mL/min. The fraction containing the product was then diluted 1:1 with water, lyophilized, and purified by HPLC as described below.

Each oligomer was purified first on a 19 mm × 150 mm Waters μBondapak C_{18} column with a gradient of 10–40% acetonitrile–0.1 M triethylammonium acetate (TEAA) in 30 min at 4 mL/min. The combined product fractions (300–700 OD_{260}) were diluted with water, lyophilized, and then detritylated by dissolving in 20 mL of water and then adding 20 mL of 0.4 M acetic acid. When the reaction was complete (10–30 min as monitored by analytical HPLC), the solution

Table I: Base Composition and Extinction Coefficients

	dC	dG	dT	dA	d(O⁶MeG)	$\epsilon_{260,25°C}$ ($\times 10^4$ M^{-1} cm^{-1})
d(GGTTATTGG)		4.0	4.0	1.0		8.18
d(GGTTCTTGG)	1.1	3.9	4.1			8.13
d(GGTTGTTGG)		5.1	3.9			8.19
d(GGTTTTTGG)		4.0	5.0			7.94
d[GGTT(O⁶Me)GTTGG]		3.9	4.1		1.0	6.60
d(CCAAAAACC)	4.0			5.0		7.06
d(CCAACAACC)	5.0			4.1		7.23
d(CCAAGAACC)	4.0	1.0		4.0		7.22
d(CCAATAACC)	4.1		1.0	3.9		7.34
d[CCAA(O⁶Me)GAACC]	4.0			4.1	1.2	7.06

was neutralized by addition of a few drops of concentrated aqueous ammonia and lyophilized.

The next purification was carried out on a 10 mm × 250 mm Beckman Ultrapure C_3 column using a gradient of 5–20% acetonitrile–0.1 M TEAA in 45 min at 2 mL/min. In several cases it was necessary to repurify some fractions on the same column. The combined product fractions (150–400 OD_{260}) were diluted 1:1 with water, lyophilized, and then desalted as described above. The lyophilized sample was converted to the sodium form using a Bio-Rad AG 50W-X2 (sodium form) ion-exchange column.

Base Composition. A 1-OD_{260} sample of each oligomer in a 400-μL polypropylene tube was lyophilized, dissolved in 80 μL of 0.1 M TEAA, pH 10, and cleaved to the deoxynucleoside level by addition of 5 μL (0.01 unit) of venom phosphodiesterase and 4 μL (4 units) of bacterial alkaline phosphatase. Each mixture was heated at 55 °C for 1 h and then analyzed by HPLC using a gradient of 2–20% acetonitrile–0.1 M TEAA in 5 min at 4 mL/min. The composition of each oligomer was determined by comparison to previously characterized molecules, d(ATGCAT) and d[CGC(O⁶Me)GCG] (Kuzmich et al., 1983), which were degraded and chromatographed under identical conditions. The numbers listed in Table I represent the average of three determinations.

Duplex Preparation. The extinction coefficients, ε, also listed in Table I were determined experimentally by phosphate analysis. A 1-OD_{260} sample of each oligomer was degraded with perchloric acid and the phosphate content determined spectrophotometrically (Snell & Snell, 1949). With these ε values, stock solutions of each oligomer were prepared in a buffer containing 10 mM sodium phosphate, 0.1 mM Na-EDTA, and 0.1 M NaCl, adjusted to pH 7.0. Mixing experiments performed on several oligomers verified that in fact a 1:1 mixture showed the greatest hypochromicity.

Optical Melting Studies. The melting curves were obtained on a Perkin-Elmer 575 spectrophotometer interfaced to a Tektronix 4051 for data acquisition and analysis. A concentrated solution of each duplex was diluted with additional 0.1 M NaCl buffer to give four samples, each with absorption values ranging from 0.4 to 1.0 at 274 nm when placed in a set of tightly stoppered cuvettes with path lengths of 1, 0.5, 0.2, and 0.1 cm. Melts were carried out at 274 nm by increasing the temperature continuously from 0 to 100 °C at a rate of 1 °C/min with a Peltier heated and cooled cell holder. A total of 400 points were measured for each cell. Samples were removed, diluted with additional buffer, and melted again to give a total of eight different concentrations per duplex, ranging from 5.7 to 200 μM. Derivative curves were obtained from a program described elsewhere (Snyder, 1985).

Results and Discussion

Synthesis

Incorporation of d(O⁶MeG) into Synthetic Oligonucleotides. As we have reported previously (Kuzmich, 1983; Gaffney, 1984a), both modification of synthetic procedures and careful purification are required for synthesis of oligonucleotides containing d(O⁶MeG). Some of our conclusions have been reiterated recently by Chambers (Borowy-Borowski & Chambers, 1987). The main hazards encountered with d(O⁶MeG) are as follows.

(1) Ammonolysis of the OMe Group To Give the 2,6-Diaminopurine Deoxyriboside. This is particularly serious in that 2,6-diaminopurine pairs strongly with thymine (Gaffney et al., 1984b) and so could substantially distort thermodynamic measurements to indicate favorable interaction with thymine. The effect on biological experiments, such as mutation rate studies, could be even more adverse. We introduced use of a solution of methanol and the nonnucleophilic base DBU as an alternative to aqueous ammonia that precludes the possibility of generation of 2,6-diaminopurine residues.

(2) Incomplete Deprotection of the 2-Amino Group of O⁶MeG Residues. This occurs because the isobutyryl group, the N^2 protecting group commonly used for protection of guanine, is cleaved from O⁶MeG exceptionally slowly, particularly in an oligonucleotide. As an alternative, to ensure that deprotection is complete, we introduced use of the more labile N^2 acetyl group (Gaffney, 1984a).

(3) Demethylation of O⁶MeG Residues To Give Guanine Residues. We noted previously that the thiophenol used in deprotection of the methyl group of the internucleotide phosphotriester moiety was capable also of slowly demethylating the O⁶MeG residues (Gaffney, 1984a). This problem can be minimized by carefully limiting the thiophenol treatment; but if as a result the methyl triesters are not completely deprotected, they will methylate thymine at the N^3 during the methanol/DBU step (Gao et al., 1985). We have now synthesized the protected d(O⁶MeG) 2-cyanoethyl phosphoramidite, so that thiophenol treatment is no longer required for deprotection.

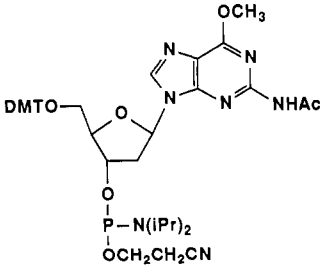

Oligonucleotide Synthesis. The set of 10 non-self-complementary nonadeoxyribonucleoside octaphosphates, d(GGTTXTTGG) and d(CCAAYAACC), where X and Y are A, C, G, T, or O⁶MeG, was synthesized by an automated phosphoramidite procedure. The syntheses were carried out on a scale of ~20 μmol of CPG–bound monomer, as described above, with 2-cyanoethyl phosphoramidite derivatives. Yields after two, or in some cases three, HPLC purifications were

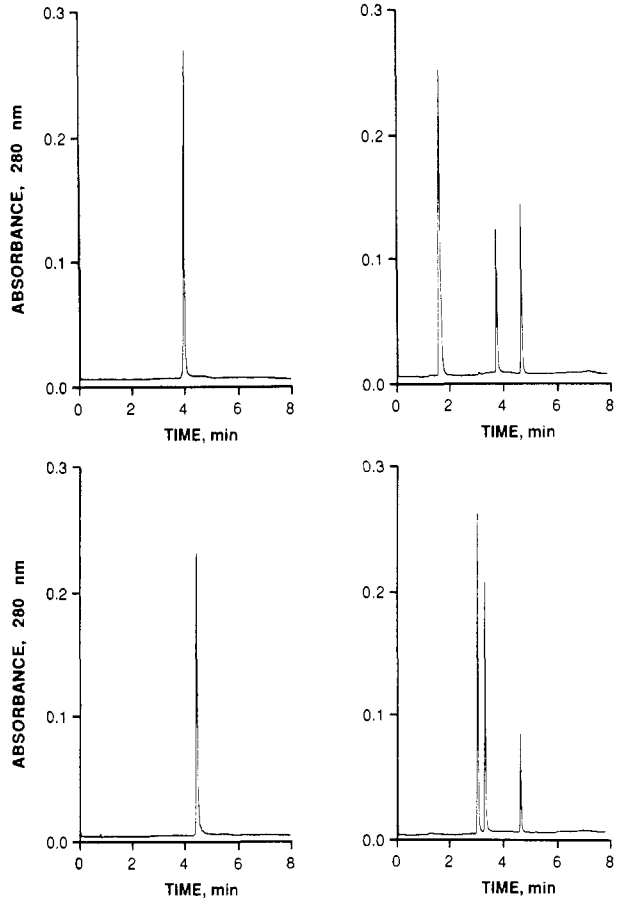

FIGURE 1: Analytical C_{18} HPLC profiles of d[CCAA(O^6Me)-GAACC] (upper) and d[GGTT(O^6Me)GTTGG] (lower) after purification (left, 5–20% CH_3CN–0.1 M TEAA at 4 mL/min) and after enzymatic degradation (right, 2–20% CH_3CN–0.1 M TEAA at 4 mL/min). The deoxynucleosides elute in the order dC, dG, dT, dA, and d(O^6MeG).

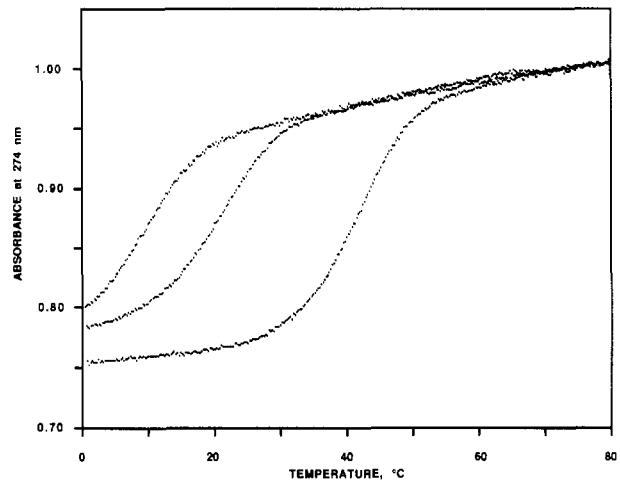

FIGURE 2: Melting curves at 274 nm for, from left to right, the C·C, O^6MeG·C, and G·C duplexes at concentrations of 25.2, 24.4, and 25.1 μM, respectively.

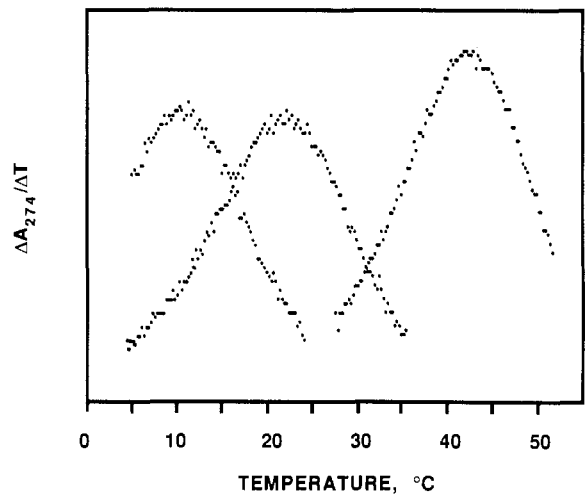

FIGURE 3: Differential melting curves for the duplexes in Figure 2.

generally in the area of 400 OD_{260} (~5 μmol). The phosphoramidites were prepared from the appropriately protected deoxynucleoside with (diisopropylamino)tetrazolide and 2-cyanoethyl *N,N,N′,N′*-tetraisopropylphosphorodiamidite (Barone et al., 1984).

Distillation of 2-Cyanoethyl Dichlorophosphite. The 2-cyanoethyl *N,N,N′,N′*-tetraisopropylphosphorodiamidite was prepared essentially by the reported procedures except that the vacuum distillations of this product and the intermediate 2-cyanoethyl dichlorophosphite (Sinha et al., 1983) were effected using a falling-film apparatus. In this apparatus the mixture to be distilled is dropped onto a glass finger, which is heated by a refluxing solvent. The vapor need only travel about 1 cm to the cool outer wall where it is condensed and collected. The unvaporized material travels the length of the hot finger and then it too is collected. The prolonged heating of the product mixture necessary during distillation of the 2-cyanoethyl dichlorophosphite with conventional apparatus tends to cause it to degrade to a pyrophoric, high-boiling material. As a result yields are variable and in our hands were generally poor. The falling-film apparatus drastically reduces the time during which the reaction mixture is heated, thereby allowing the distillation to be effected without concomitant degradation.

Final Detritylation. One change from the procedures we have published previously is that we no longer use 80% acetic acid for the last detritylation (between HPLC purifications). We have found that much more dilute solutions of acetic acid (0.1–0.2 M, pH ~3.5) are just as effective. Detritylation is complete in 20–40 min (by HPLC). The mixture is then neutralized by addition of a few drops of aqueous ammonia and concentrated, or lyophilized, as desired. This procedure is both milder and more convenient than is use of 80% acetic acid.

Purity. The product oligonucleotides were all homogeneous by HPLC, under the conditions described above. In addition, the composition of each was verified by HPLC analysis of the mixture of deoxynucleosides produced upon enzymatic cleavage (Table I). The HPLC profiles obtained for the two molecules containing O^6MeG are shown in Figure 1.

Optical Melting Studies

This set of non-self-complementary oligonucleotides can be mixed in pairs to produce 4 normal Watson–Crick duplexes and 21 duplexes with a single mismatch, of which 9 contain O^6MeG. Figure 2 shows three typical melting curves, corresponding to the highest and lowest melting duplexes and an O^6MeG duplex. Because many of the curves do not have a sufficient lower base line to calculate accurately the T_m, we used T_{max}, the highest point on the derivative curve, as the measure of duplex stability (Gralla & Crothers, 1973; Albergo et al., 1981; Marky & Breslauer, 1987). The T_{max} for a given transition is generally within 1 deg of the T_m but is not identical with it. Figure 3 shows melting curves, differentiated incrementally with respect to temperature, for the same duplexes shown in Figure 2.

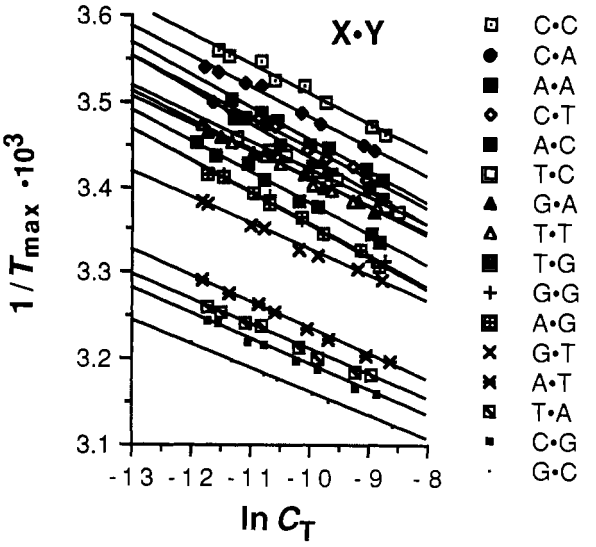

FIGURE 4: Plots of $1/T_{max}$ versus ln concentration, C_T, for duplexes which do not contain O⁶MeG. Listed in order from the highest to lowest T_{max}: G·C; C·G; T·A; A·T; G·T; A·G; G·G; T·G; T·T; G·A; T·C; A·C; C·T; A·A; C·A; C·C.

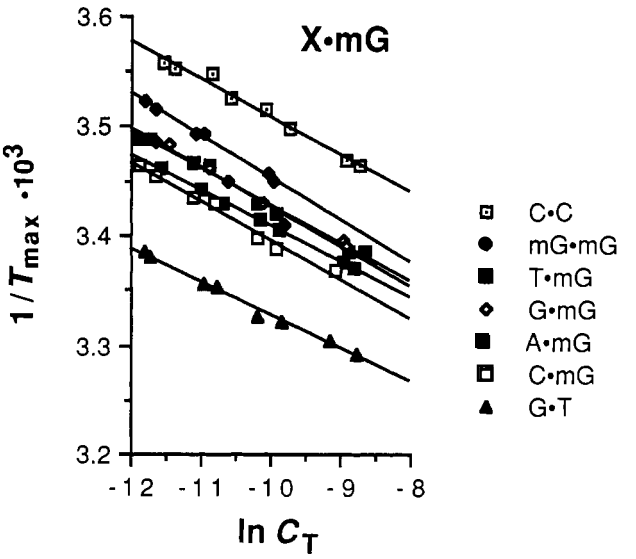

FIGURE 5: Plots of $1/T_{max}$ versus ln concentration, C_T, for duplexes which contain X·O⁶MeG pairs, along with G·T and C·C duplexes, for comparison. Listed in order from the highest to lowest T_{max}: G·T; C·O⁶MeG; A·O⁶MeG; G·O⁶MeG; T·O⁶MeG; O⁶MeG·O⁶MeG; C·C.

For non-self-complementary molecules, the equilibrium constant K for formation of a duplex from single strands, assuming a two-state model, can be written as

$$K = 2\alpha/[C_T(1 - \alpha)^2] \quad (1)$$

where α is defined as the fraction of total strands in the duplex state and C_T is the total concentration in single strands (Breslauer, 1986). It can be shown that, for a bimolecular process, at the T_{max}, $\alpha = 0.41$ (Gralla & Crothers, 1973; Albergo et al., 1981). Assuming that $\Delta H°$ and $\Delta S°$ are independent of temperature, substitution in eq 2 and rearrangement leads to eq 3:

$$\Delta G° = \Delta H° - T\Delta S° = -RT \ln K \quad (2)$$

$$\frac{1}{T_{max}} = \frac{R}{\Delta H°} \ln C_T + \frac{\Delta S° - 1.8}{\Delta H°} \quad (3)$$

This equation corresponds to a straight line, $y = mx + b$, where $y = 1/T_{max}$, the slope $m = R/\Delta H°$, $x = \ln C_T$, and the intercept $b = (\Delta S° - 1.8)/\Delta H°$. For each duplex, a plot of $1/T_{max}$ vs ln C_T gave a straight line (see supplementary material) from which $\Delta H°$, $\Delta S°$, and $\Delta G°$ were calculated. This treatment assumes that the transitions being monitored are two state. This assumption is reasonable for these nonamers, on the basis of both their length and their sequence (Breslauer, 1986). Moreover, since T_{max} is relatively insensitive to stateness, the effect of small deviations from two-state behavior on the enthalpy and entropy derived from these $1/T_{max}$ vs ln C_T plots should be minimal.

Figure 4 shows plots of $1/T_{max}$ vs ln C_T for combinations in which X·Y corresponds to pairs and mismatched pairs of the standard deoxynucleosides. Figures 5 and 6 show analogous plots where X or Y, or both, is O⁶MeG, along with, for comparison, C·C and G·T pairs, respectively the least and most thermally stable of the mismatches. The relative order of thermal stability of the O⁶MeG pairs seen here is consistent with the other O⁶MeG-containing molecules that we have studied previously, in which O⁶MeG was flanked by C on both the 5′ and 3′ sides. The O⁶MeG pair with C is thermally more stable than is the pair with T, whether O⁶MeG is in the X strand, where the flanking base is T, or is in the Y strand, where the flanking base is A.

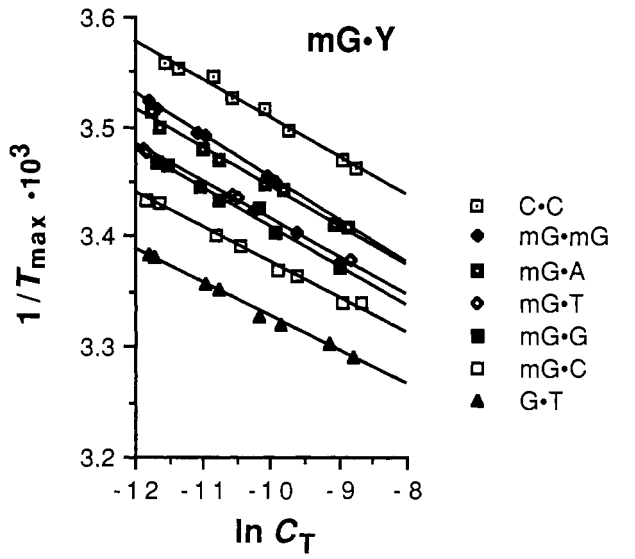

FIGURE 6: Plots of $1/T_{max}$ versus ln concentration, C_T, for duplexes which contain O⁶MeG·Y pairs, along with G·T and C·C duplexes, for comparison. Listed in order from the highest to lowest T_{max}: G·T; O⁶MeG·C; O⁶MeG·G; O⁶MeG·T; O⁶MeG·A; O⁶MeG·O⁶MeG; C·C.

This set of molecules also allows the first comparison of O⁶MeG pairs to normal base mismatches. Figures 4–6 show, qualitatively, that the O⁶MeG pairs have a relatively narrow range of thermal stabilities, lying roughly in the middle of the range of thermal stabilities seen for the mismatches. The thermodynamic properties tabulated in Table II, together with the free energy differences, $\Delta\Delta G°$, listed in Table III, give a more quantitative comparison. Thus, for example, in the X strand, where the flanking bases are thymine, replacing the guanine of a G·C base pair with O⁶MeG causes a 4.5 kcal/mol decrease in thermal stability, which is seen to be (Table II) largely enthalpic in origin. This O⁶MeG·C pair is 0.9 kcal/mol less stable than the corresponding G·T mispair but is 0.6 kcal/mol more stable than the G·A mispair and is more stable by 0.7–2.0 kcal/mol than any of the X·C mispairs. The O⁶MeG·T pair is 5.1 kcal/mol less stable than a G·C pair and 1.5 kcal/mol less stable than a G·T mispair. The T·T mispair is 0.2 kcal/mol more stable, and the C·T mispair is 0.3 kcal/mol less stable than the O⁶MeG·T pair.

Table II: Thermodynamic Properties

G-G-T-T-X-T-T-G-G
C-C-A-A-Y-A-A-C-C

X·Y	T_{max} (°C) (10^{-4} M)[a]	$\Delta H°$ (kcal/mol)[b]	$\Delta S°$ [kcal/(mol·deg)][c]	$\Delta G°_{25°C}$ (kcal/mol)[d]	X·Y	T_{max} (°C) (10^{-4} M)[a]	$\Delta H°$ (kcal/mol)[b]	$\Delta S°$ [kcal/(mol·deg)][c]	$\Delta G°_{25°C}$ (kcal/mol)[d]
G·C	45.4	−71	−0.20	−10.5	A·A	18.8	−53	−0.16	−4.8
C·G	42.5	−67	−0.19	−9.8	C·A	16.4	−56	−0.17	−4.2
T·A	40.7	−68	−0.20	−9.4	C·C	14.2	−57	−0.18	−3.9
A·T	38.2	−66	−0.19	−8.7	^{m}G·C	25.2	−63	−0.19	−5.9
G·T	29.6	−65	−0.19	−6.9	^{m}G·G	22.6	−56	−0.17	−5.4
A·G	27.5	−53	−0.16	−6.5	^{m}G·T	21.9	−58	−0.18	−5.3
G·G	27.3	−54	−0.16	−6.3	^{m}G·A	19.4	−56	−0.17	−4.8
T·G	25.2	−54	−0.16	−6.1	C·^{m}G	23.8	−56	−0.17	−5.6
T·T	22.5	−58	−0.18	−5.5	A·^{m}G	22.4	−61	−0.19	−5.5
G·A	22.4	−61	−0.19	−5.3	G·^{m}G	21.2	−54	−0.16	−5.4
T·C	21.5	−61	−0.19	−5.1	T·^{m}G	21.0	−58	−0.18	−5.3
A·C	20.7	−51	−0.15	−5.3	^{m}G·^{m}G	19.0	−52	−0.16	−4.8
C·T	19.5	−56	−0.17	−5.0					

[a] Estimated precision ±0.3 °C. [b] Estimated precision ±2 kcal/mol. [c] Estimated precision ±10 cal/(mol·deg). [d] Estimated precision ±0.1 kcal/mol.

Table III: $\Delta\Delta G°_{25°C}$ (kcal/mol)[a]

d[GGTTXTTGG]·d[CCAAYAACC]

X·Y	^{m}G·C	^{m}G·G	^{m}G·T	^{m}G·A	C·^{m}G	A·^{m}G	G·^{m}G	T·^{m}G	^{m}G·^{m}G	C·C	C·A	A·A	C·T	A·C	T·C	G·A	T·T	T·G	G·G	A·G	G·T	A·T	T·A	C·G
G·C	4.5	5.1	5.1	5.7	4.9	4.9	5.1	5.1	5.7	6.5	6.3	5.7	5.5	5.2	5.3	5.1	4.9	4.4	4.2	4.0	3.6	1.8	1.1	0.7
C·G	3.8	4.3	4.4	4.9	4.1	4.2	4.4	4.4	5.0	5.8	5.5	5.0	4.7	4.5	4.6	4.4	4.2	3.7	3.5	3.3	2.9	1.1	0.4	
T·A	3.4	4.0	4.0	4.5	3.8	3.8	4.0	4.0	4.6	5.4	5.1	4.6	4.4	4.1	4.2	4.0	3.8	3.3	3.1	2.9	2.5	0.7		
A·T	2.7	3.3	3.3	3.8	3.1	3.1	3.3	3.3	3.9	4.7	4.4	3.9	3.7	3.4	3.5	3.3	3.1	2.6	2.4	2.2	1.8			
G·T	0.9	1.5	1.5	2.0	1.3	1.3	1.5	1.5	2.1	2.9	2.6	2.1	1.9	1.6	1.7	1.5	1.3	0.8	0.6	0.4				
A·G	0.5	1.1	1.2	1.7	0.9	1.0	1.1	1.2	1.7	2.6	2.3	1.7	1.5	1.2	1.4	1.2	1.0	0.4	0.2					
G·G	0.4	0.9	1.0	1.5	0.7	0.8	0.9	1.0	1.5	2.4	2.1	1.5	1.3	1.0	1.2	1.0	0.8	0.2						
T·G	0.2	0.7	0.8	1.3	0.5	0.6	0.7	0.8	1.3	2.2	1.9	1.3	1.1	0.8	1.0	0.8	0.6							
T·T	−0.4	0.1	0.2	0.7	−0.1	0.0	0.1	0.2	0.7	1.6	1.3	0.7	0.5	0.3	0.4	0.2								
G·A	−0.6	−0.1	0.0	0.5	−0.3	−0.2	−0.1	0.0	0.6	1.4	1.1	0.5	0.3	0.1	0.2									
T·C	−0.8	−0.3	−0.2	0.3	−0.5	−0.4	−0.3	−0.2	0.4	1.2	0.9	0.3	0.1	−0.1										
A·C	−0.7	−0.1	−0.1	0.5	−0.3	−0.3	−0.1	−0.1	0.5	1.4	1.1	0.5	0.3											
C·T	−0.9	−0.4	−0.3	0.2	−0.6	−0.5	−0.4	−0.3	0.2	1.1	0.8	0.2												
A·A	−1.2	−0.6	−0.5	0.0	−0.8	−0.7	−0.6	−0.5	0.0	0.9	0.6													
C·A	−1.7	−1.2	−1.1	−0.6	−1.4	−1.3	−1.2	−1.1	−0.6	0.3														
C·C	−2.0	−1.5	−1.4	−0.9	−1.7	−1.6	−1.5	−1.4	−0.9															
^{m}G·^{m}G	−1.2	−0.6	−0.5	0.0	−0.8	−0.8	−0.6	−0.5																
T·^{m}G	−0.6	−0.1	0.0	0.5	−0.3	−0.2	−0.1																	
G·^{m}G	−0.6	0.0	0.1	0.6	−0.2	−0.1																		
A·^{m}G	−0.4	0.1	0.2	0.7	−0.1																			
C·^{m}G	−0.3	0.2	0.3	0.8																				
^{m}G·A	−1.1	−0.6	−0.5																					
^{m}G·T	−0.6	−0.1																						
^{m}G·G	−0.5																							

[a] These $\Delta\Delta G°$ values are the difference between the $\Delta G°$ values of the horizontal and vertical X·Y duplexes ($\Delta G°_{h} - \Delta G°_{v}$) and were determined before rounding off $\Delta G°$ to the numbers listed in Table II.

The trend for molecules with O^{6}MeG in the Y strand, where the flanking bases are adenine, is roughly the same. The C·O^{6}MeG pair is 4.1 kcal/mol less stable than the C·G pair but is more stable (by 0.6–1.7 kcal/mol) than any of the C·Y mispairs. The T·O^{6}MeG pair is 4.4 kcal/mol less stable than the C·G pair and 0.8 kcal/mol less stable than the T·G mispair. The T·T mispair is 0.2 kcal/mol more stable and the T·C mispair is 0.2 kcal/mol less stable than the T·O^{6}MeG pair. Furthermore, a comparison of O^{6}MeG in the X and Y strands shows that there is no free energy difference between the T·O^{6}MeG and O^{6}MeG·T pairs or between the G·O^{6}MeG and O^{6}MeG·G pairs and only a 0.3 kcal/mol difference between the C·O^{6}MeG and O^{6}MeG·C pairs. The only substantial difference is seen for the A·O^{6}MeG pair, which is more stable than O^{6}MeG·A by 0.7 kcal/mol. In contrast, each of the Watson–Crick pairs shows a 0.7 kcal/mol difference, and the normal base mispairs, except for T·C/C·T, show even larger differences. The O^{6}MeG pairs thus appear to be much less sensitive to sequence effects than are either normal base pairs or mispairs.

There have been several reports in recent years dealing with mismatch stability (Aboul-ela et al., 1985; Martin et al., 1985; Werntges et al., 1986; Kawase et al., 1986; Eritja et al., 1986a; Ikuta et al., 1987). The thermodynamic properties found were, in general, quite consistent with those of the Watson–Crick pairs and normal base mispairs that we report here. The thermodynamic study of duplexes of sequence d[CAAAX-AAAG]·d[CTTTYTTTG], where X and Y are A, C, G, or T (Aboul-ela et al., 1985), is the most closely analogous set to the one we have used. Our work, however, was done at 0.1 rather than 1 M NaCl and used T_{max} rather than T_m. In both sets the most stable mispairs are those containing guanine, while the least stable are those containing cytosine. The only differences are in the relative order of duplexes which are of very similar thermal stabilities. Moreover, in each set when the X·Y pair involves adenine, there is in one of the duplexes a strand with a consecutive run of A's: seven in the Tinoco series and five in ours. As was noted by these authors, the properties of such molecules may be more analogous to those of dA_n·dT_n, where unique structures, including "bent" structures, are possible (Koo & Crothers, 1988), than to those of a more heterogeneous sequence. In both sets the A·T duplex with the run of A's was thermally *more* stable. In the Tinoco series this molecule was, narrowly, the second most stable duplex. Conversely, again in both series, both the A·G mispair and the A·C mispair were thermally *less* stable when there was a run of A's in the duplex. This also holds in the present set for the O^{6}MeG·A pair, where the duplex with the run of A's is thermally less stable by 0.7 kcal/mol. As noted above, this is the only instance where there is a substantial sequence dependence for an O^{6}MeG pair. In our earlier work with the dodecamers d[CGNGAATTC(O^{6}Me)GCG], the relative order of stability was C > A > G > T. This order holds here as well, except for the set in which there is a duplex with five A's. This is the least stable duplex in the set, and the order then becomes C > G > T > A.

A similar order of mismatch stability was found in a study of the dissociation kinetics of 19-mer duplexes containing single mismatches, even though the mismatch site was flanked by G·C pairs (Ikuta et al., 1987). From these results, it was hypothesized that mispairs were more stable when there was the possibility of H-bonding between a thymine N^3 imido proton or a guanine N^1 amido proton, which are commonly referred to as "imino" protons, and an imino nitrogen in the opposite base. The O^{6}MeG pairs do not fit this hypothesis.

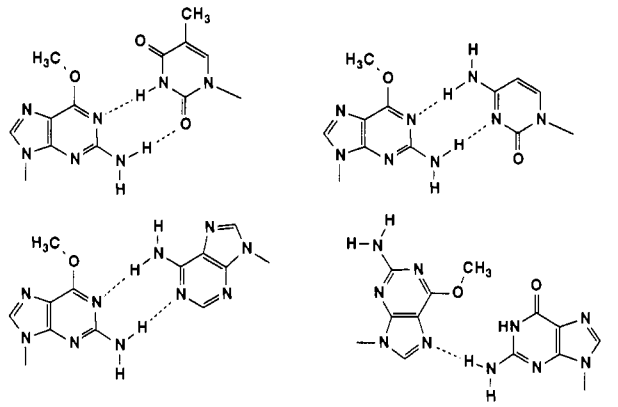

FIGURE 7: Possible base pairing schemes for O^{6}MeG.

In all duplexes we have studied to date the most stable O^{6}MeG pair is with cytosine, in which such H-bonding is not possible, at least not without tautomerization. A possible explanation for these results, which would be consistent with the ^{1}H NMR (Patel et al., 1986b), is that the *O*^{6}-methyl group may sterically prevent H-bonding between the thymine N^3 imido proton and the O^{6}MeG N^1 imino nitrogen.

The $\Delta\Delta G°$ values listed in Table III for O^{6}MeG pairs show only a 1.1 kcal/mol difference between the most and least thermally stable pairs, O^{6}MeG·C and O^{6}MeG·A, respectively. If the latter is excluded because of the five consecutive A's, the difference becomes only 0.6 kcal/mol. Moreover, in the X·O^{6}MeG set the difference among the four pairs is only 0.3 kcal/mol. This weak discrimination by O^{6}MeG gives it the potential to be useful for ambiguous positions in probes. It is less discriminatory toward all four bases than is, for example, deoxyinosine toward three (Martin et al., 1985; Kawase et al., 1986; Eritja et al., 1986b). But O^{6}MeG is probably too destabilizing to be used at more than one or two sites in a probe, which severely limits its potential. Despite this minimal specificity of O^{6}MeG in a duplex, there is substantial specificity in the polymerase complex, where the O^{6}MeG clearly codes for thymine (or uracil). This is not a case where a weak thermodynamic interaction is enhanced in the polymerase complex but rather a case where an opposite specificity is created. Of the possible O^{6}MeG pairs that are suggested by the ^{1}H NMR (Figure 7), the O^{6}MeG·T pair most closely approximates Watson–Crick geometry. The pairs with A and C may be wobble pairs, while the pair with G has the O^{6}MeG in a syn conformation. Moreover, the ^{31}P chemical shift dispersion for the O^{6}MeG·T duplex was most like that of the unmodified molecule, which also may be indicative of a more normal, B-DNA structure for this duplex. If the most stable O^{6}MeG duplex structures contain conformations that are not allowed by the active site, the duplexes cannot serve as models of the structure in the polymerase complex, and thermodynamic measurements based on the duplex then cannot approximate the coding properties of O^{6}MeG.

There is other recent evidence that supports such discrimination by the active site. The imperfect correlation between nucleotide insertion by DNA polymerase α opposite either xanthine or 2-aminopurine and the thermal stability of the corresponding duplexes has been explained on this basis (Eritja et al., 1986b; Fazakerley et al., 1987). Furthermore, from a comparison of thermal melting and enzyme kinetic measurements involving normal base mispairs, it was suggested that the enzyme binding cleft snugly fits correct base pairs and excludes water, in order to amplify free energy differences to achieve the observed specificity (Petruska et al., 1988). It is possible that only pairs which closely approximate Watson–

Crick pairs would be allowed by such a close-fitting active site. Thus the more stable O^6MeG pairs, which all may involve deviation from Watson–Crick spatial relationships, may not fit such a site. The less stable, but perhaps less distorted pair with thymine may be better accommodated. It has been reported that the O^6MeG·C pair may have a Watson–Crick type of geometry, but only after protonation of the cytosine N^3, which presumably occurs only after duplex formation and so could not stabilize the polymerase complex (Williams & Shaw, 1987).

The results reported above confirm our previous findings regarding the relative stability of O^6MeG base pairs and provide the first comparison of O^6MeG pairs with normal base mispairs. The O^6MeG pairs were found to lie in about the middle of the range of thermal stabilities of the mispairs. In contrast to the mispairs, the O^6MeG pairs display little sequence dependence and differ much less in thermal stability. This very weak discrimination by O^6MeG could make it useful in probes, although the poor thermal stability of the O^6MeG pairs is limiting. The striking difference between these duplex thermal stabilities and the known coding preferences of O^6MeG is consistent with the Tinoco and Goodman model for exclusion by the polymerase active site of pairs which differ substantially from Watson–Crick geometry. The slightly greater thermal stability of O^6MeG pairs with C, A, and G, relative to that of T, may therefore be irrelevant to the processes of replication or transcription, since the C, A, and G pairs all may involve decidedly non-Watson–Crick spatial relationships. It should be noted that the H-bonding of the O^6MeG pairs shown in Figure 7 was only inferred from the ^{1}H NMR; it was not observed directly. In order to define the H-bonding present in duplexes containing O^6MeG, and perhaps in the polymerase complex as well, we are pursuing experiments based upon introduction of ^{15}N to the 1, 2, and 7-positions of *O*^{6}-methyldeoxyguanosine.

Acknowledgments

We thank Dr. Kenneth J. Breslauer for helpful discussions and for use of his laboratory facilities (GM 23509) and Doris Hartenthaler for performing the phosphate analyses.

Supplementary Material Available

Line equations for ln C_T vs $1/T_{max}$ plots (1 page). Ordering information is given on any current masthead page.

Registry No. d(GGTTATTGG), 121030-77-1; d(GGTTCTTGG), 121030-78-2; d(GGTTGTTGG), 121030-79-3; d(GGTTTTTGG), 121030-80-6; d[GGTT(O^6Me)GTTGG], 121030-81-7; d(CCAAAAACC), 121030-82-8; d(CCAACAACC), 121055-38-7; d(CCAAGAACC), 121030-83-9; d(CCAATAACC), 121030-84-0; d[CCAA(O^6Me)GAACC], 121072-49-9; 2-cyanoethyl *N,N,N',N'*-tetraisopropylphosphorodiamidite, 102691-36-1; phosphorus trichloride, 7719-12-2; 3-hydroxypropionitrile, 109-78-4; 2-cyanoethyl dichlorophosphite, 76101-30-9; diisopropylamine, 108-18-9.

References

Abbott, P. J., & Saffhill, R. (1978) *Biochim. Biophys. Acta 562*, 51–61.

Aboul-ela, F., Koh, D., Tinoco, I., Jr., & Martin, F. H. (1985) *Nucleic Acids Res. 13*, 4811–4824.

Albergo, D. D., Marky, L. A., Breslauer, K. J., & Turner, D. H. (1981) *Biochemistry 20*, 1409–1413.

Barone, A. D., Tang, J.-Y., & Caruthers, M. H. (1984) *Nucleic Acids Res. 12*, 4051–4061.

Belinsky, S. A., White, C. M., Devereus, T. R., Swenberg, J. A., & Anderson, M. W. (1987) *Cancer Res. 47*, 1143–1148.

Bhanot, O. S., & Ray, A. (1986) *Proc. Natl. Acad. Sci. U.S.A. 83*, 7348–7352.

Borowy-Borowski, H., & Chambers, R. W. (1987) *Biochemistry 26*, 2465–2471.

Breslauer, K. J. (1986) in *Thermodynamic Data for Biochemistry and Biotechnology* (Hinz, H.-J., Ed.) Chapter 15, pp 402–407, Springer-Verlag, New York.

Briscoe, W. T., & Cotter, L. E. (1985) *Chem.-Biol. Interact. 56*, 321–331.

Caldwell, J. W., & Kollman, P. A. (1985) *J. Biomol. Struct. Dyn. 3*, 57–66.

Chambers, R. W., Sledziewska-Gojska, E., Hirani-Hojatti, S., & Borowy-Borowski, H. (1985) *Proc. Natl. Acad. Sci. U.S.A. 82*, 7173–7177.

Domoradzki, J., Pegg, A. E., Dolan, M. E., Maher, V. M., & McCormick, J. J. (1984) *Carcinogenesis 5*, 1641–1647.

Eritja, R., Kaplan, B. E., Mhaskar, D., Sowers, L. C., Petruska, J., & Goodman, M. F. (1986a) *Nucleic Acids Res. 14*, 5869–5884.

Eritja, R., Horowitz, D. M., Walker, P. A., Ziehler-Martin, J. P., Boosalis, M. S., Goodman, M. F., Itakura, K., & Kaplan, B. E. (1986b) *Nucleic Acids Res. 14*, 8135–8154.

Fazakerley, G. V., Sowers, L. C., Eritja, R., Kaplan, B. E., & Goodman, M. F. (1987) *Biochemistry 26*, 5641–5646.

Gaffney, B. L., Marky, L. A., & Jones, R. A. (1984a) *Biochemistry 23*, 5686–5691.

Gaffney, B. L., Marky, L. A., & Jones, R. A. (1984b) *Tetrahedron 40*, 3–13.

Gao, X., Gaffney, B. L., Senior, M., Riddle, R. R., & Jones, R. A. (1985) *Nucleic Acids Res. 13*, 573–584.

Gerson, S. L., Trey, J. E., Miller, K., & Benjamin, E. (1987) *Cancer Res. 47*, 89–95.

Gralla, J., & Crothers, D. M. (1973) *J. Mol. Biol. 78*, 301–319.

Grunberger, D., & Singer, B. (1983) *Molecular Biology of Mutagens and Carcinogens*, Plenum, New York.

Hill-Perkins, M., Jones, M. D., & Karran, P. (1986) *Mutat. Res. 162*, 153–163.

Ikuta, S., Takagi, K., Wallace, R. B., & Itakura, K. (1987) *Nucleic Acids Res. 15*, 797–811.

Kawase, Y., Iwai, S., Inoue, H., Miura, K., & Ohtsuka, E. (1986) *Nucleic Acids Res. 14*, 7727–7736.

Klopman, G., & Ray, A. (1982) *Cancer Biochem. Biophys. 6*, 31–35.

Koo, H.-S., & Crothers, D. M. (1988) *Proc. Natl. Acad. Sci. U.S.A. 85*, 1763–1767.

Kuzmich, S., Marky, L. A., & Jones, R. A. (1983) *Nucleic Acids Res. 11*, 3393–3404.

Lawley, P. D., Harris, G., Phillips, E., Irving, W., Colaço, C. B., Lydyard, P. M., & Roitt, I. M. (1986) *Chem.-Biol. Interact. 57*, 107–121.

Loechler, E. L., Green, C. L., & Essigman, J. M. (1984) *Proc. Natl. Acad. Sci. U.S.A. 81*, 6271–6275.

Loveless, A. (1969) *Nature (London) 223*, 206–207.

Lucchesi, P., Carraway, M., & Marinus, M. G. (1986) *J. Bacteriol. 166*, 34–37.

Marky, L. A., & Breslauer, K. J. (1987) *Biopolymers 26*, 1601–1620.

Martin, F. H., Castro, M. M., Aboul-ela, F., & Tinoco, I., Jr. (1985) *Nucleic Acids Res. 13*, 8927–8938.

Mehta, J. R., & Ludlum, D. B. (1978) *Biochim. Biophys. Acta 521*, 770–778.

Nagata, C., Takeda, E., & Aida, M. (1982) *Mutat. Res. 105*, 1–8.

Patel, D. J., Shapiro, L., Kozlowski, S., Gaffney, B. L., & Jones, R. A. (1986a) *Biochemistry 25*, 1027–1036.
Patel, D. J., Shapiro, L., Kozlowski, S., Gaffney, B. L., & Jones, R. A. (1986b) *Biochemistry 25*, 1037–1042.
Patel, D. J., Shapiro, L., Kozlowski, S., Gaffney, B. L., & Jones, R. A. (1986c) *J. Mol. Biol. 188*, 1–16.
Petruska, J., Goodman, M. F., Boosalis, M. S., Sowers, L. C., Cheong, C., & Tinoco, I., Jr. (1988) *Proc. Natl. Acad. Sci. U.S.A. 85*, 6252–6256.
Richardson, K. K., Richardson, F. C., Crosby, R. M., Swenberg, J. A., & Skopek, T. R. (1987) *Proc. Natl. Acad. Sci. U.S.A. 84*, 344–348.
Sinha, N. D., Biernat, J., & Köster, H. (1983) *Tetrahedron Lett. 24*, 5843–5846.
Snell, F. D., & Snell, C. T. (1949) *Colorimetric Methods of Analysis, Vol.* 2, p 671, Van Nostrand, New York.
Snyder, J. G. (1985) Ph.D. Thesis, Rutgers University.
Ti, G. S., Gaffney, B. L., & Jones, R. A. (1982) *J. Am. Chem. Soc. 104*, 1316–1319.
Topal, M. D., Eadie, J. S., & Conrad, M. (1986) *J. Biol. Chem. 261*, 9879–9885.
Werntges, H., Steger, G., Riesner, D., & Fritz, H.-J. (1986) *Nucleic Acids Res. 14*, 3773–3790.
Williams, L. D., & Shaw, B. R. (1987) *Proc. Natl. Acad. Sci. U.S.A. 84*, 1779–1783.
Zarbl, H., Sukumar, S., Arthur, A. V., Martin-Zanca, D., & Barbacid, M. (1985) *Nature (London) 315*, 382–385.

Subtilisin-Cleaved Actin: Polymerization and Interaction with Myosin Subfragment 1†

Deborah Schwyter, Martin Phillips, and Emil Reisler*
Department of Chemistry and Biochemistry and Molecular Biology Institute, University of California, Los Angeles, California 90024

Received January 25, 1989; Revised Manuscript Received March 27, 1989

ABSTRACT: Homogeneous preparations of actin cleaved into two fragments, the N-terminal 9- and C-terminal 36-kDa peptides, were achieved by proteolysis of G-actin with subtilisin at 23 °C at a 1:1000 (w/w) ratio of enzyme to actin. The subtilisin cleavage site was identified by sequence analysis to be between Met-47 and Gly-48. Although under nondenaturing conditions the two fragments remained associated to one another, the cleavage affected macromolecular interactions of actin. The rates of cleaved actin polymerization by $MgCl_2$, KCl, and myosin subfragment 1 (S-1) were slower and the critical concentrations for this process were higher than in intact protein. Intact and cleaved actin formed morphologically indistinguishable filaments and copolymerized in the presence of $MgCl_2$. The affinity of actin for S-1 was decreased by about 10-fold due to subtilisin cleavage, but the S-1 ATPase activity was activated to the same V_{max} value by both intact and cleaved actins. DNase I inhibition measurements revealed lower affinity of cleaved actin for DNase I than that of intact protein. These results are discussed in terms of actin's structure.

The interactions of actin with a large number of proteins are central to its function in motile processes in nonmuscle cells, polymerization into filaments, and the contraction of muscle (Korn, 1982). The interest in these interactions has stimulated studies on structure–function relationships and the mapping of protein binding sites on actin. The N-terminal segment on actin attracted particular attention in these investigations. Chemical cross-linking with carbodiimide revealed that the N-terminal acidic residues on actin could be covalently linked to myosin subfragment 1 (S-1)[1] (Mornet et al., 1981; Sutoh, 1982), troponin I (Grabarek & Gergely, 1987), tropomyosin (Grabarek et al., 1988), and several additional proteins (Sutoh & Hatano, 1986). Although the functional implications of these findings are yet to be fully clarified, they point to the importance of the N-terminal segment in the interactions of actin with a number of proteins.

Other studies, including chemical modifications of residues located between His-40 and Tyr-69 (Hegyi et al., 1974; Lehrer & Elzinga, 1972; Bender et al., 1976; Burtnick, 1984), focused primarily on the significance of this region in actin–actin interactions. They demonstrated variable degrees of inhibition of actin polymerization by probes attached to specific residues in that segment of the protein.

The mapping of functional sites on proteins is frequently facilitated by their proteolytic fragmentation and, if feasible, the separation of protein fragments. Two sites on G-actin were recently shown to exhibit general protease sensitivity (Mornet & Ue, 1984). The first one was detected in earlier work which showed tryptic cleavage of actin at Lys-68 (Jacobson & Rosenbusch, 1976). The resulting 33-kDa "core" fragment had lost two important functional properties of actin: the polymerization into filaments and the binding to myosin (Jacobson & Rosenbusch, 1976; Konno, 1988). The second site, closer to the N-terminus of actin, was detected through the proteolytic formation of a 35-kDa fragment of actin (Mornet & Ue, 1984). A chymotryptic cut at that site, between Met-44 and Val-45, yields a protein split into 10- and 35-kDa fragments and appears to have a much smaller effect on the properties of actin than the cleavage at the 33-kDa site (Konno, 1987). The split actin retained its ability to polymerize and bind to

† This work was supported by U.S. Public Health Service Grant AR 22031 and by National Science Foundation Grant DMB 85-08507.
* Address correspondence to this author at the Department of Chemistry and Biochemistry, University of California.

[1] Abbreviations: S-1, myosin subfragment 1; EDTA, ethylenediaminetetraacetic acid; IAF, 5-(iodoacetamido)fluorescein; PMSF, phenylmethanesulfonyl fluoride.

0006-2960/89/0428-5889$01.50/0